

Nonlinear vibrations of loudspeaker-like structures

Nicolas Quaegebeur*, Antoine Chaigne

UME-ENSTA, Chemin de la Humière, 91761 Palaiseau Cedex, France

Received 23 October 2006; received in revised form 2 March 2007; accepted 11 June 2007
Available online 14 September 2007

Abstract

During high amplitudes of vibration, nonlinearities affect the electroacoustical behavior of electrodynamic transducers and are responsible for audible distortions. We distinguish two types of nonlinearities: electrical and mechanical. In this study, attention is paid to the mechanical and geometrical properties of loudspeaker-like structures. The loudspeaker is viewed as a combination of an annular plate with a circular plate. Nonlinear vibrations of such a structure are investigated, using the dynamic analog of the Von-Kármán equations. Furthermore, the influence of both material properties and geometrical parameters is studied. It is shown that nonlinear effects can be substantially reduced by choosing appropriate material and geometrical parameters.

© 2007 Elsevier Ltd. All rights reserved.

1. Introduction

The aim of an electrodynamic loudspeaker is to transform an electrical signal into sound. Such a transduction is expected to be linear. However, for high levels of vibrations, nonlinear phenomena appear and are responsible for audible distortions. The various sources of nonlinearities can be separated into two parts [1]: “electrical” nonlinearities due to the large displacement of the coil in the permanent magnet, and “mechanical” nonlinearities due to large displacements of the moving parts of the system. The classical model for electrical and mechanical nonlinearities consists of a lumped parameters model, which holds the simplifying assumption that the vibration pattern can be reduced to a single rigid-body mode [2]. Previous experimental studies reported in the literature have shown that mechanical and geometrical properties of the system can significantly influence the response of the loudspeaker [3–5]. However, only a few number of proposed models include the influence of material in the electroacoustical transduction. Former studies propose a lumped model approach [6], a continuous mechanical model [7], or finite elements models [8], all of which are restricted to the linear domain. In the present paper, the goal is to extend these results by considering the influence of geometrical nonlinearities. Since the transformation of mechanical vibrations into sound in air is linear, the present study is limited to the vibratory problem.

The loudspeaker is viewed here as the combination of an annular plate together with a circular plate (see Fig. 1). We leave the effects of curvature and of more complex geometries (conical shells) for future studies.

*Corresponding author. Tel.: +33 1 69 31 99 20.

E-mail address: nicolas.quaegebeur@ensta.org (N. Quaegebeur).

Nomenclature			
a	external radius	ε	dimensionless nonlinear parameter
b	radius of the inner part	μ_p	dimensionless damping for mode p
E	Young's modulus	ν	Poisson's ratio
F	force function	ρ	density
h	thickness	σ	ratio of densities
s	ratio of inner and outer diameters	Φ_p	p th natural mode for the flexural displacement
T_p	external loads for mode p	Ψ_p	p th natural mode for the force function
$u(r, t)$	longitudinal displacement	ω_p	dimensionless modal (angular) frequency for mode p
$w(r, t)$	transverse displacement	\mathcal{M}	bending moment
γ	ratio of longitudinal rigidities	\mathcal{N}	membrane forces
δ	ratio of flexural rigidities	\mathcal{Q}	transverse shear force

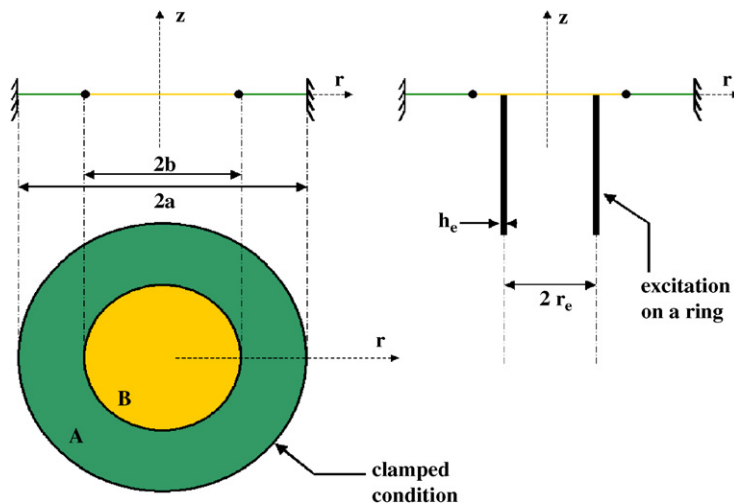


Fig. 1. (Left) Geometry of the system under study. (Right) A typical example of studied loading. Both structures A and B have different material properties and the junction is supposedly lossless.

Linear and nonlinear vibrations of both annular and circular plates have been widely investigated in the past (see Refs. [9–13] for linear models and [14–18] for nonlinear models). Analytical solutions can be obtained for particular cases of boundary conditions. However, the association of an annular suspension with a central structure has been less documented. As far as we are aware, only the case where the central structure is rigid has been treated [9,19–24]. In the present study, the dynamic analog of the Von-Kármán equations is used to include geometrical nonlinearities in the local vibration equations, taking into account the stretching of the mid-plane of the structure. The influence of material properties and of geometrical parameters on linear and nonlinear vibrations is expressed in terms of dimensionless parameters. The solutions of the problem are expanded on the linear modes of the structure which yield the nonlinear differential equations of the dimensionless problem. The influence of dimensionless terms on both the modal frequencies and nonlinear parameters is studied. It is shown that, in order to reduce geometrical nonlinearities, the ratio between the inner and the outer diameters between the suspension and the central diaphragm must be as small as possible and that material properties for the cone structure be carefully selected.

2. Description of the simplified loudspeaker

2.1. Geometry of the problem

The system is composed of a circular plate B attached to an annular structure A . The total radius is denoted by a and A is clamped at its outer edge (where $r = a$). The junction between A and B is located at $r = b$ (see Fig. 1 for more details).

The two structures have different Young's moduli E_A and E_B , Poisson's ratio ν_A and ν_B , thickness h_A and h_B , density ρ_A and ρ_B , and different damping properties.

2.2. Assumptions

The system is assumed to be invariant by rotation around the axis of revolution z . This assumption results from the axisymmetric excitation of the loudspeaker. Experimental observations on loudspeakers show that the asymmetric modes can generally be neglected.

The junction between both plates is supposed to be lossless. Continuity of both the transverse and longitudinal displacement, and of the forces and of the bending moments is assumed to occur at this junction (where $r = b$).

We assume the Von-Kàrmàn theory for vibration of plates. As mentioned by Nayfeh [16,17], this formulation offers a correction to the linear small deflection theory. Mathematically, the validity of this approach is restricted to displacements such that $w \propto h^2/a$, but in fact, it yields good results even for amplitudes of displacement comparable to the thickness h of the structure [26]. The underlying assumptions of this model are the following:

- The structure is thin: $h/a \ll 1$.
- The Kirchhoff–Love assumptions are verified.
- Only nonlinear terms of the lowest order are kept in the expression of strains as a function of the displacement.
- The in-plane and rotatory inertia terms are neglected.

In the present study, the reaction of the surrounding fluid on the structure is neglected, thus the excitation forces are the only external forces.

3. Formulation of the problem

3.1. Local equations

Let $w(r, t)$ denote the transverse displacement at point r and time t . The dynamic analog of the Von-Kàrmàn equations, with addition of damping and external load on the structure B , are written as [14]

for $0 < r < b$:

$$\begin{aligned} D_B \Delta \Delta w + m_B \ddot{w} &= L(w, F) - c_B \dot{w} + T(r, t), \\ \Delta \Delta F &= -\frac{E_B h_B}{2} L(w, w). \end{aligned} \quad (1)$$

for $b < r < a$:

$$\begin{aligned} D_A \Delta \Delta w + m_A \ddot{w} &= L(w, F) - c_A \dot{w}, \\ \Delta \Delta F &= -\frac{E_A h_A}{2} L(w, w), \end{aligned} \quad (2)$$

where in the axisymmetric case, we have

$$L(u, v) = v_{,rr} \frac{u_{,r}}{r} + u_{,rr} \frac{v_{,r}}{r},$$

$$D = \frac{Eh^3}{12(1 - \nu^2)}: \text{flexural rigidity,}$$

$$m = \rho h: \text{surface density,}$$

$$T(r, t): \text{external forces exerted on the central structure.}$$

$(\star)_{,r}$ and $\dot{(\star)}$ denote the derivatives with respect to spatial coordinate r and time t . The Laplacian in cylindrical coordinates is written as

$$\Delta(\star) = (\star)_{,rr} + \frac{1}{r}(\star)_{,r}.$$

In Eqs. (1) and (2), the linear approach cancels the force function, which means $F = 0$. The usual notations for the moments \mathcal{M} and for the transverse forces \mathcal{Q} with respect to coordinate r are the following:

$$\mathcal{M} = -D \left(w_{,rr} + \frac{\nu}{r} w_{,r} \right),$$

$$\mathcal{Q} = -D(\Delta w)_{,r},$$

where the membrane forces \mathcal{N} with respect to coordinate r in the axisymmetrical case and the longitudinal displacement u are:

$$u = \frac{\gamma \mathcal{N}}{Eh} = \frac{F_{,rr}}{Eh} (rF_{,rr} - \nu F_{,r}).$$

3.2. Boundary conditions

The structure A is clamped at $r = a$, which means

$$u(a, t) = 0,$$

$$w(a, t) = 0,$$

$$\frac{\partial w}{\partial r}(a, t) = 0. \tag{3}$$

The condition of continuity for the displacement field at the junction between A and B (in $r = b$) is written as

$$w(b^+, t) = w(b^-, t),$$

$$u(b^+, t) = u(b^-, t),$$

$$\frac{\partial w}{\partial r}(b^+, t) = \frac{\partial w}{\partial r}(b^-, t). \tag{4}$$

The continuity of the moments and the transverse forces yields

$$\mathcal{M}(b^+, t) = \mathcal{M}(b^-, t),$$

$$(\mathcal{Q} + \mathcal{N} w_{,r})(b^+, t) = (\mathcal{Q} + \mathcal{N} w_{,r})(b^-, t). \tag{5}$$

3.3. Nondimensional form of the equations

Eqs. (1) and (2) are written in nondimensional form with respect to the external structure A :

$$r = (a)\bar{r}, \quad t = \left(a^2 \sqrt{\frac{m_A}{D_A}} \right) \bar{t}, \quad w = \left(\frac{h_A^2}{a} \right) \bar{w},$$

$$F = \left(\frac{E_A h_A^5}{a^2} \right) \bar{F}, \quad c = 2 \left(\frac{E_A h_A^5}{a^4} \sqrt{\frac{m_A}{D_A}} \right) \bar{\mu}, \quad T = \left(\frac{E_A h_A^7}{a^7} \right) \bar{T}.$$

For $0 < r < s$:

$$\begin{aligned} \frac{\delta}{\sigma} \Delta \Delta w + \ddot{w} &= \frac{\varepsilon}{\sigma} (L(w, F) - 2\sigma \mu_B \dot{w} + T), \\ \Delta \Delta F &= -\frac{\gamma}{2} L(w, w). \end{aligned} \quad (6)$$

For $s < r < 1$:

$$\begin{aligned} \Delta \Delta w + \ddot{w} &= \varepsilon (L(w, F) - 2\mu_A \dot{w}), \\ \Delta \Delta F &= -\frac{1}{2} L(w, w), \end{aligned} \quad (7)$$

where the useful dimensionless variables for our problem are:

$$\begin{aligned} \sigma &= \frac{\rho_B h_B}{\rho_A h_A}, \\ \delta &= \frac{E_B h_B^3}{E_A h_A^3} \frac{1 - \nu_A^2}{1 - \nu_B^2}, \quad s = \frac{b}{a}, \\ \gamma &= \frac{E_B h_B}{E_A h_A}, \quad \varepsilon = 12(1 - \nu_A^2) \frac{h_A^2}{a^2}. \end{aligned} \quad (8)$$

The parameter σ represents the density ratio between both structures. The parameters δ and γ denote the flexural rigidity and the longitudinal rigidity ratio between both structures, respectively. In Eqs. (6) and (7), it appears that δ and σ are related to the linear system, while γ has an influence on the force function F only. The relative magnitude of the nonlinear terms are related to the value of ε and, finally, s represents the geometrical aspect ratio of the structure.

The dimensionless boundary conditions for the problem become

$$\begin{aligned} u(1, t) = 0, \quad w(1, t) = 0, \quad \frac{\partial w}{\partial r}(1, t) = 0, \\ w(s^+, t) = w(s^-, t), \quad u(s^+, t) = \gamma u(s^-, t), \quad \frac{\partial w}{\partial r}(s^+, t) = \frac{\partial w}{\partial r}(s^-, t), \\ \mathcal{M}(s^+, t) = \delta \mathcal{M}(s^-, t), \quad (\mathcal{Q} + \mathcal{N}w_r)(s^+, t) = \delta(\mathcal{Q} + \mathcal{N}w_r)(s^-, t). \end{aligned} \quad (9)$$

The last boundary condition contains a condition for the displacement w and for the force function F . In the linear range, the force function tends to zero and the condition can be linearized. In the general case, this condition correlates transverse and longitudinal displacements. The order of magnitude of the two terms \mathcal{Q} and $\mathcal{N}w_r$ are evaluated by using the dimensionless equations:

$$(\mathcal{Q} + \mathcal{N}w_r)(s^+, t) = \delta(\mathcal{Q} + \mathcal{N}w_r)(s^-, t)$$

and

$$\left(w_{,rrr} - \frac{w_{,rr}}{r} + \frac{w_{,r}}{r^2} (1 + \varepsilon r^2 F_{,rr}) \right) (s^+, t) = \delta \left(w_{,rrr} - \frac{w_{,rr}}{r} + \frac{w_{,r}}{r^2} (1 + \varepsilon r^2 F_{,rr}) \right) (s^-, t). \quad (10)$$

Considering that $\varepsilon \ll 1$, the term $(\varepsilon r^2 F_{,rr})$ can be neglected with respect to unity. Eq. (10) can then be linearized and reduced to

$$\mathcal{Q}(s^+, t) = \delta \mathcal{Q}(s^-, t). \quad (11)$$

In summary, the problem takes the following dimensionless form for $r \in [0 : 1]$

$$\begin{aligned} \frac{\delta}{\sigma}(r)\Delta\Delta w + \ddot{w} &= \varepsilon \left(\frac{1}{\sigma(r)}L(w, F) - 2\sigma(r)\mu(r)\dot{w} + T(r, t)\frac{1}{\sigma(r)} \right), \\ \Delta\Delta F &= -\frac{\gamma(r)}{2}L(w, w). \end{aligned} \tag{12}$$

where

	$0 < r < s$	$s < r < 1$
$\sigma(r)$	σ	1
$\delta(r)$	δ	1
$\gamma(r)$	γ	1
$\mu(r)$	μ_B	μ_A

and the boundary conditions are:

$$\begin{aligned} u(1, t) = 0, \quad w(1, t) = 0, \quad \frac{\partial w}{\partial r}(1, t) = 0, \\ u(s^+, t) = \gamma u(s^-, t), \quad w(s^+, t) = w(s^-, t), \quad \frac{\partial w}{\partial r}(s^+, t) = \frac{\partial w}{\partial r}(s^-, t), \\ \mathcal{M}(s^+, t) = \delta \mathcal{M}(s^-, t), \quad \mathcal{Q}(s^+, t) = \delta \mathcal{Q}(s^-, t). \end{aligned} \tag{13}$$

Eq. (12) is analogous to the plate theory when $\sigma = \delta = \gamma = 1$ and $\mu_A = \mu_B$ (in this limiting case, both structures have the same material properties). To solve this nonlinear PDE, the solutions are then expanded to the linear modes of the structures.

4. Modal expansion

4.1. Transverse displacement

The transverse displacement of the structure is expanded onto the linear modes as follows:

$$w(r, t) = \sum_{p=0}^{\infty} \Phi_p(r)q_p(t). \tag{14}$$

As a consequence of Eq. (14) the nonlinear terms are contained in the temporal part of the solution. The mathematical properties of the eigenmodes $\Phi_p(r)$ are found in Appendix A.2. Both the modal shapes Φ_p and frequencies ω_p depend on the dimensionless parameter:

$$\mathcal{L} = \left(\frac{\sigma}{\delta} \right)^{1/4}$$

This parameter represent the mass/stiffness ratio of the compound system.

4.2. Force function $F(r, t)$

Again, the force function is expanded onto the linear modes [15]:

$$F(r, t) = \sum_{l=0}^{\infty} \Psi_l(r)\eta_l(t), \tag{15}$$

where the functions $\Psi_l(r)$ are the modal shapes. As a consequence, Eq. (12) yields for $0 < r < s$:

$$\Delta\Delta F(r, t) = \sum_{l=0}^{\infty} \Delta\Delta\Psi_l(r)\eta_l(t) = -\frac{\gamma}{2} \sum_p \sum_q L(\Phi_p, \Phi_q)q_pq_q \tag{16}$$

for $s < r < 1$:

$$\Delta\Delta F(r, t) = \sum_{l=0}^{\infty} \Delta\Delta\Psi_l(r)\eta_l(t) = -\frac{1}{2} \sum_p \sum_q L(\Phi_p, \Phi_q)q_pq_q, \tag{17}$$

and the boundary conditions become

$$\begin{aligned} \Psi_{p,rrr}(1) + \Psi_{p,rr}(1) - \Psi_{p,r}(1) &= 0, & \Psi_p(1) &= 0, & \Psi_{p,rr}(1) - v_S\Psi_{p,r}(1) &= 0, \\ [\Psi_{p,rrr}(s^+) + \Psi_{p,rr}(s^+) - \Psi_{p,r}(s^+)]_{s^-}^{s^+} &= 0, & \Psi_p(s^+) &= \Psi_p(s^-), \\ \Psi_{p,rr}(s^+) - \frac{v_B}{s}\Psi_{p,r}(s^+) &= \gamma\left(\Psi_{p,rr}(s^-) - \frac{v_B}{s}\Psi_{p,r}(s^-)\right). \end{aligned} \tag{18}$$

For $0 < r < s$, Ψ_p must satisfy

$$\Delta\Delta\Psi_p = \gamma\xi_p^4\Psi_p, \tag{19}$$

where for $s < r < 1$:

$$\Delta\Delta\Psi_p = \xi_p^4\Psi_p. \tag{20}$$

The solutions for $0 < r < s$ are:

$$\Psi_p(r) = Q_{1p}J_0(\xi_p\mathcal{F}r) + Q_{2p}I_0(\xi_p\mathcal{F}r),$$

and for $s < r < 1$:

$$\Psi_p(r) = Q_{3p}J_0(\xi_p r) + Q_{4p}Y_0(\xi_p r) + Q_{5p}I_0(\xi_p r) + Q_{6p}K_0(\xi_p r),$$

where (I_0 , J_0 , K_0 and Y_0) are the standard Bessel functions (see Appendix A.2). The dimensionless parameter \mathcal{F} is defined as

$$\mathcal{F} = \gamma^{1/4}. \tag{21}$$

Finally, from Eq. (12), we obtain

$$\begin{aligned} \Delta\Delta F &= \sum_b \Delta\Delta\Psi_b(r)\eta_b(t), \\ &= \gamma \sum_b \xi_b^4\Psi_b(r)\eta_b(t), \\ &= -\frac{\gamma(r)}{2} \sum_p \sum_q L(\Phi_p, \Phi_q)q_p(t)q_q(t). \end{aligned} \tag{22}$$

Using the orthogonality property of functions Ψ_p gives

$$\xi_b^4\eta_b(t) = -\frac{1}{2} \sum_p \sum_q \iint_S L(\Phi_p, \Phi_q)\Psi_b \, dS q_p(t)q_q(t)$$

and, after normalization of the modal shapes, the force function F is written

$$F = -\frac{1}{2} \sum_b \sum_p \sum_q \Psi_b \mathcal{G}_{pqb} q_p(t)q_q(t), \tag{23}$$

where

$$\mathcal{G}_{pqb} = \frac{\iint_S \gamma L(\Phi_p, \Phi_q) \Psi_b \, dS}{\xi_b^4 \iint_S \Psi_b^2 \, dS}.$$

4.3. Mechanical equations of the problem

We now introduce the modal expansions of the displacement and force functions into Eq. (12). Using again the orthogonality properties of the modal shapes, one obtains the following system of nonlinearly coupled differential equations:

$$\omega_a^2 q_a + \ddot{q}_a = \varepsilon \left(\sum_p \sum_q \sum_u \Gamma_{pqau} q_p q_q q_u - 2\mu_a \dot{q}_a + T_a \right), \tag{24}$$

where

$$\omega_a^2 = \frac{\iint_S \frac{\delta}{\sigma}(r) \Phi_a \Delta \Delta \Phi_a \, dS}{\iint_S \Phi_a^2 \, dS} = \frac{\delta}{\sigma} \int_0^s \Phi_a \Delta \Delta \Phi_a r \, dr + \int_s^1 \Phi_a \Delta \Delta \Phi_a r \, dr, \tag{25}$$

$$\mu_a = \frac{\iint_S \mu(r) \Phi_a^2 \, dS}{\iint_S \Phi_a^2 \, dS} = \mu_B \int_0^s \Phi_a^2 r \, dr + \mu_A \int_s^1 \Phi_a^2 r \, dr, \tag{26}$$

$$T_a = \frac{\iint_S \frac{\Phi_a T}{\sigma(r)} \, dS}{\iint_S \Phi_a^2 \, dS} = \frac{1}{\sigma} \int_0^s \Phi_a T r \, dr, \tag{27}$$

$$\Gamma_{pqau} = \frac{1}{2} \sum_b \frac{\iint_S \gamma(r) L(\Phi_p, \Phi_q) \Psi_b \, dS \iint_S \frac{L(\Phi_u, \Psi_b) \Phi_a}{\sigma(r)} \, dS}{\xi_b^4 \iint_S \Psi_b^2 \, dS \iint_S \Phi_a^2 \, dS}, \tag{28}$$

$$= \frac{1}{2 \xi_b^4} \sum_b \iint_S \gamma(r) L(\Phi_p, \Phi_q) \Psi_b \, dS \iint_S \frac{L(\Phi_u, \Psi_b) \Phi_a}{\sigma(r)} \, dS. \tag{29}$$

The eigenfrequencies ω_a are given by the sum of the two terms that illustrate the respective influences on both parts *A* and *B* of the structures. For a loudspeaker, the first eigenfrequency (called the rigid body mode in the electroacoustical community) must be chosen to be as low as possible, whereas the other eigenfrequencies must be chosen to be as high as possible in order to extend the bandwidth where the transducer works as a rigid piston. This ensures, among other things, that the radiation pattern is not affected by the upper modes of the diaphragm.

The damping factor μ_a for any given mode *a* depends on both the damping constants of the materials used in the structure, with a weighting factor from the modal shapes. For a loudspeaker, the damping must be sufficiently high in order to avoid the presence of resonances that would alter the reproduced sound. In our simulations, values of $\mu_A = 0.8$ and $\mu_B = 0.2$ were chosen, in accordance with typical values measured on loudspeakers.

4.4. Forcing terms

In a real electrodynamic transducer, the structure is excited by a coil moving in the magnetic field of a permanent magnet. In what follows, the coil is viewed as a rigid cylindrical shell of width h_e glued to the diaphragm at position $r = r_e$ (see Fig. 1).

The well-known equation that governs electromechanical transduction is

$$U_e(t) = R_E I(t) + L_E \frac{dI}{dt} + BIV(t), \tag{30}$$

where $U_e(t)$ is the input electrical signal, $I(t)$ is the intensity of the current in the coil, R_E and L_E are the resistance and the self inductance of the coil, and Bl is the force factor. V denotes the velocity of the diaphragm on the circle where $r = r_e$. Electrical nonlinearities are not considered here.

Using the modal expansion, under the assumption that $h_e/r_e \ll 1$, we have

$$V(t) = \sum_p \Phi_p(r_e) \dot{q}_p(t).$$

The equation of motion for the coil is

$$M_E \dot{V}(t) = BlI(t) - T(r, t), \quad (31)$$

where M_E represents the mass of the coil and $T(r, t)$ denotes the external forces on the structure. Using the results presented in the previous sections, the projection of $T(r, t)$ onto any mode a reads

$$\begin{aligned} T_a &= \frac{1}{\sigma} \int_0^s \Phi_a T(r, t) r dr, \\ &= - \left(\frac{2a^7 r_e h_e \Phi_a(r_e)}{E_A h_A^7 \sigma(r_e)} \right) \left(M_E \sum_p \Phi_p(r_e) \ddot{q}_p(t) - Bl I(t) \right). \end{aligned} \quad (32)$$

This formulation shows that the modal driving force depends on both the inertia of the coil and the driving current. It is commonly admitted that the inertia of the coil is small so that its corresponding term can be neglected with respect to the electrical force term $Bl I(t)$. As a consequence, it can be assumed that

$$T_a \simeq \left(\frac{2a^7 r_e h_e \Phi_a(r_e)}{E_A h_A^7 \sigma(r_e)} \right) Bl I(t). \quad (33)$$

Eq. (33) shows, in particular, that the modal forcing term is proportional to the modal shape at the point of excitation and to the intensity of the current.

5. Application to loudspeakers

5.1. Limiting cases of the model

In this section, the influence of the material and geometrical properties of the diaphragm on its vibration pattern is investigated. Let s characterize the geometry and δ , γ and σ characterize the material properties (see Section 3). We distinguish two limiting cases of interest:

- $\delta = 1$: This corresponds to the situation where the elastic properties are similar in both parts of the structure. The same modal shapes are obtained for all values of σ and s , but the values of the modal frequencies vary with the density ratio σ . In this case, our results are comparable to existing results in the literature [9,16].
- $\delta \gg 1$: In that case, the structure B is significantly more rigid than the annular structure A . Therefore, the deformations mostly affect the outer structure A , corresponding to the standard behavior of loudspeakers in low-frequency range (piston-like case). Numerical results in the linear range can be found in Refs. [9,19].

The modal shapes obtained with our model for the first three modes of vibration, in these two limiting cases are presented in Table 1. We select the geometrical parameter $s = 0.5$ and the density ratio $\sigma = 1$. The dimensionless damping factors are $\mu_A = 0.8$ (rubber) and $\mu_B = 0.1$ (steel).

5.2. Validation of the model

When both structures are identical, the solution reduces to the plate case. Table 2 compares the results obtained with our model to previous results published by Nayfeh [16]. The results present a comparison between modal frequencies ω_a and nonlinear coefficients Γ_{aaaa} (see Eq. (24)), exhibiting congruence between the two methods. Note that in this case, the calculations performed with our model are independent of the geometrical parameter s .

Table 1

Modal shapes for the first three modes in two limiting cases. For each mode a , the dimensionless eigenfrequency is noted ω_a with its corresponding damping factor μ_a in parentheses. Calculations have been performed for a density ratio $\sigma = 1$

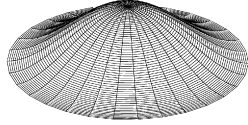
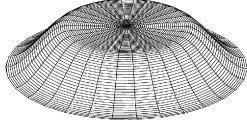
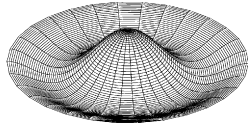
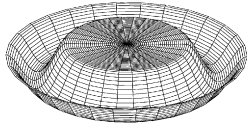
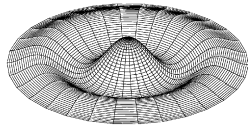
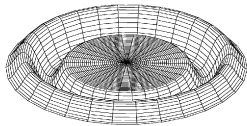
	$\delta = 1$	(damping %)	$\delta = 10^6$	(damping %)
Mode 1	$\omega_1^2 = 10.21$	(0.23)	$\omega_1^2 = 17.69$	(0.41)
				
Mode 2	$\omega_2^2 = 39.77$	(0.49)	$\omega_2^2 = 101.70$	(0.68)
				
Mode 3	$\omega_3^2 = 89.10$	(0.41)	$\omega_3^2 = 260.34$	(0.74)
				

Table 2

Comparison of the first four eigenfrequencies and nonlinear coefficients obtained using Eqs. (25) and (28) with the results from Nayfeh in Ref. [16] for a circular plate

Mode a	ω_a^2 Simulation	ω_a^2 Nayfeh	$3 \Gamma_{aaaa}$ Simulation	$3 \Gamma_{aaaa}$ Nayfeh
1	10.2158	10.2158	162.21	162.22
2	39.7711	39.7710	5552.0	5552.1
3	89.1041	89.1040	34360	34401
4	158.1842	158.1830	122190	

Other studies on vibration of annular plates with a central rigid mass were performed by Leissa and Cohen [9,19]. These authors investigated the linear vibrations of such structures for different values of s . A comparison between the first modal frequency obtained by Leissa and with the present model in the case where all materials have the same density and a stiffness ratio of $\delta = 10^6$ is presented in Table 3. Once again, excellent agreement is found, hence validating the present formulation.

5.3. Linear regime

The influence of parameters δ and σ on the values of the first three eigenfrequencies are presented in Figs. 2–4. The boundaries for those two parameters are chosen regarding existing material properties [25]

Table 3

Comparison of the first eigenfrequency ω_1 obtained using Eq. (25) for $\delta = 10^6$ with results from Leissa [9] in the case of a rigid central structure with different values of the geometrical parameter s

s	0.1	0.3	0.5	0.7	0.9
ω_1^2 Simulation	10.43	12.39	17.69	33.98	161.10
ω_1^2 Leissa	10.37	12.53	17.89	33.99	160.78

The errors between both models are below 1%.

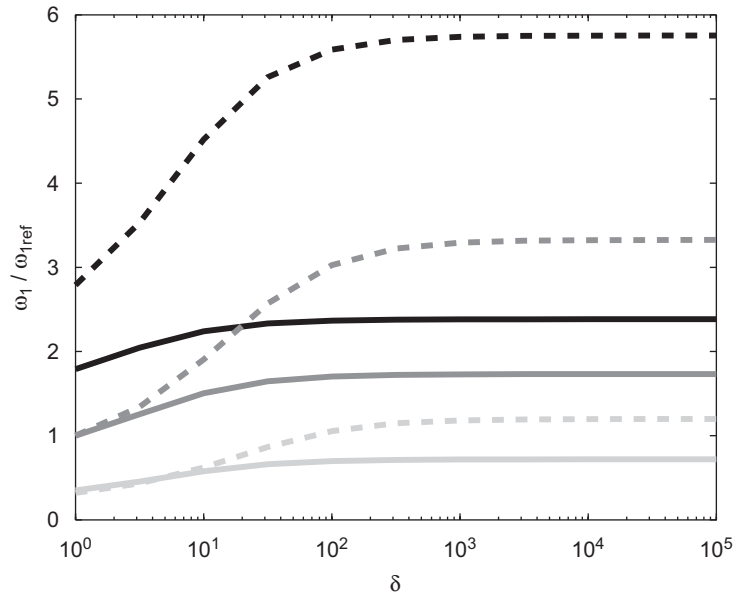


Fig. 2. Evolution of the first modal angular frequency ω_1 with respect to the flexural rigidity ratio between outer and inner structures δ for different values of density ratio σ . Black lines represent the case where $\sigma = 0.1$, dark gray lines for when $\sigma = 1$ and light gray lines for when $\sigma = 10$. The results are normalized by the value ω_{1ref} obtained in the limiting case where $\delta = \sigma = 1$. The dashed curves (— —) stand for the case $s = 0.9$ and the solid curves for the case $s = 0.7$. For $\delta < 10^2$, ω_1 increases with respect to δ and for $\delta > 10^3$, ω_1 only varies with σ and s and is independent of the rigidity ratio δ . Large values of geometrical parameter s allow to reach higher eigenfrequencies for the first mode.

when both structures have the same thickness. In the case of loudspeakers, the aim is to reach high amplitudes of vibration for a given input force. This is the reason why the outer annular structure is made of a very flexible material (elastomer). Under this consideration, the stiffness ratio δ between the outer and the inner structure can be chosen to be between 1 and 10^5 and the density ratio σ between 0.1 and 10.

Figs. 2–4 represent the evolution of dimensionless eigenfrequencies with respect to stiffness ratio δ for 3 different values of density ratio σ and 2 different values of geometrical parameter s . All the results are normalized by the value obtained in the case $\delta = \sigma = 1$. For all figures, the dashed curves stand for the case $s = 0.9$ and the solid curves for the case $s = 0.7$; black lines represent the case where $\sigma = 0.1$, dark gray lines for when $\sigma = 1$ and light gray lines for when $\sigma = 10$.

The interpretation of these results differ for the first mode (Fig. 2). Two trends can be outlined:

- for $\delta < 100$, ω_1 increases with respect to δ . This effect is amplified in the case where $s = 0.9$ (very thin suspension);

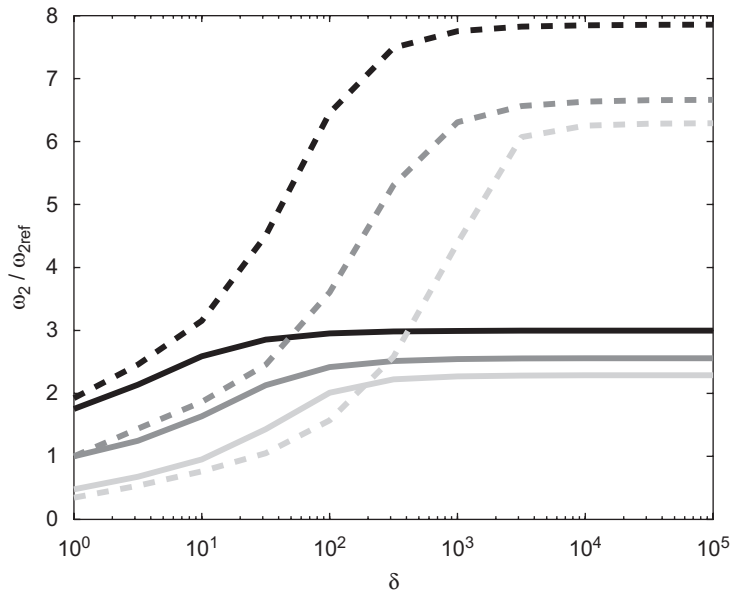


Fig. 3. Evolution of the second modal angular frequency ω_2 with respect to the flexural rigidity ratio between outer and inner structures δ for different values of density ratio σ . Black lines represent the case where $\sigma = 0.1$, dark gray lines for when $\sigma = 1$ and light gray lines for when $\sigma = 10$. The results are normalized by the value ω_{2ref} obtained in the limiting case where $\delta = \sigma = 1$. The dashed curves (—) stand for the case $s = 0.9$ and the solid curves for the case $s = 0.7$. For $\delta > 1000$, ω_2 is independent of δ and for $\delta < 100$ it can be shown that isolines of ω_2 are defined by $\delta \propto \sigma$. Large values of geometrical parameter s increase the value of the second eigenfrequency ω_2 : for $\delta > 1000$, $\omega_2 \simeq 8\omega_{2ref}$ for $s = 0.9$ when $\omega_2 \simeq 2\omega_{2ref}$ for $s = 0.7$.

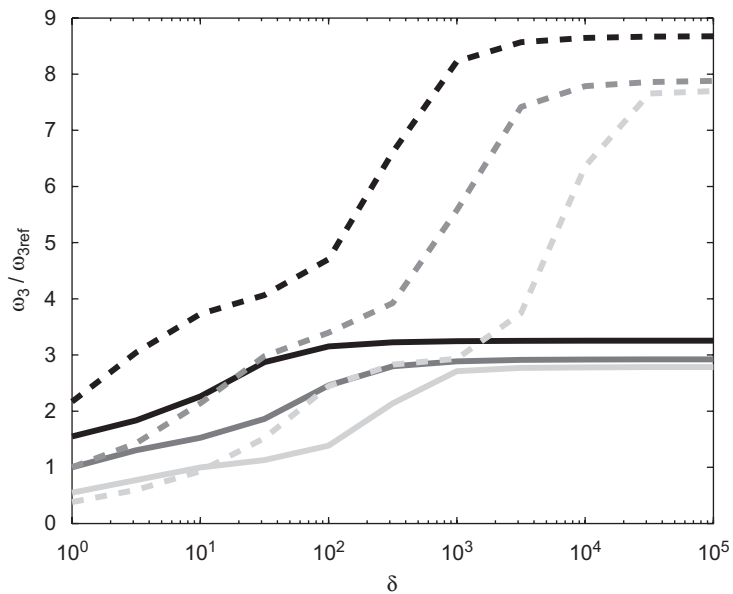


Fig. 4. Evolution of the third modal angular frequency ω_3 with respect to the flexural rigidity ratio between outer and inner structures δ for different values of density ratio σ . Black lines represent the case where $\sigma = 0.1$, dark gray lines for when $\sigma = 1$ and light gray lines for when $\sigma = 10$. The results are normalized by the value ω_{3ref} obtained in the limiting case where $\delta = \sigma = 1$. The dashed curves (—) stand for the case $s = 0.9$ and the solid curves for the case $s = 0.7$. It can be shown that for $\delta < 100$, the isolines of function ω_3 are defined by $\delta \propto \sigma$. Large values of geometrical parameter s increase the third eigenfrequency ω_3 : for $\delta > 1000$, $\omega_3 \simeq 8\omega_{3ref}$ for $s = 0.9$ when $\omega_3 \simeq 3\omega_{3ref}$ for $s = 0.7$.

- for $\delta > 100$, the values of ω_1 in Fig. 2 are independent of δ . This shows that, for high stiffness ratios, only the mass ratio σ and the geometrical ratio s have an influence on the first modal frequency.

For higher modes of vibration, it can be shown (not representable on Figs. 3 and 4) that the isolines of eigenfrequencies are defined by $\delta \propto \sigma$ for $\delta < 100$. That means that under this consideration, only the ratio mass/stiffness is of interest for predicting the eigenfrequencies of the system.

Returning to the loudspeaker case, it has been previously mentioned that the most favorable situation is obtained when the first mode is well separated from the other modes. The first modal frequency must be chosen to be as low as possible, since the electroacoustical transduction is efficient for frequencies above this mode. In addition, the other vibrational modes should be ideally situated above the audible range (i.e. for frequencies higher than 20 kHz). Based on the results shown in Figs. 2–4, it can be seen that this configuration is ideally reached when $\sigma = 10$ (where the first eigenfrequency few increases) and $\delta > 100$ (where the other eigenfrequencies largely increase).

For example, when $\delta = 10^5$ and $\sigma = 10$ and for a geometrical parameter of $s = 0.9$, the first modal frequency is not shifted but higher mode frequencies are shifted by a factor larger than 6.

5.4. Nonlinear behaviour

The nondimensional parameter ε fixes the relative amplitude of the nonlinear terms in Eq. (24). For large amplitudes of vibration, all modes are coupled through the terms Γ_{pqau} . However, for standard loudspeakers, experimental observations [2,4] show that nonlinearities give rise to harmonics in the response of the system (harmonic distortion). Internal mode coupling, where energy is transferred from one mode to another, has not been observed in our experiments. Thus, the main nonlinear effect is produced by the term $\Gamma_{aaaa}q_a^3$ (which gives rise to harmonic terms in the nonlinear response of mode a) and not by cross coupling terms Γ_{apqr}

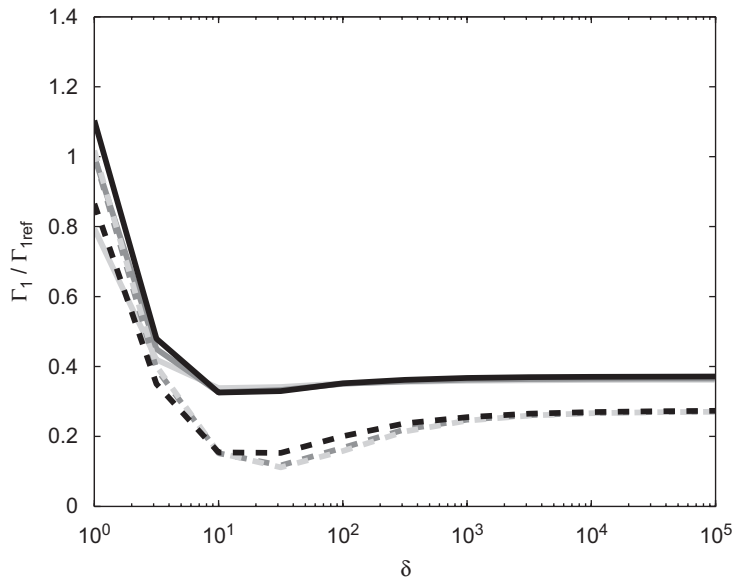


Fig. 5. Evolution of the first nonlinear coefficient Γ_{1111} with respect to the flexural rigidity ratio between outer and inner structures δ for different values of density ratio σ . Black lines represent the case where $\sigma = 0.1$, dark gray lines for when $\sigma = 1$ and light gray lines for when $\sigma = 10$. The results are normalized by the value Γ_{1ref} obtained in the limiting case where $\delta = \sigma = 1$. The dashed curves (— —) stand for the case $s = 0.9$ and the solid curves for the case $s = 0.7$. The first nonlinear coefficient is independent of the density ratio σ and a minimum is reached for $\delta = 30$. The first nonlinear coefficient decreases when the geometrical parameter s increases.

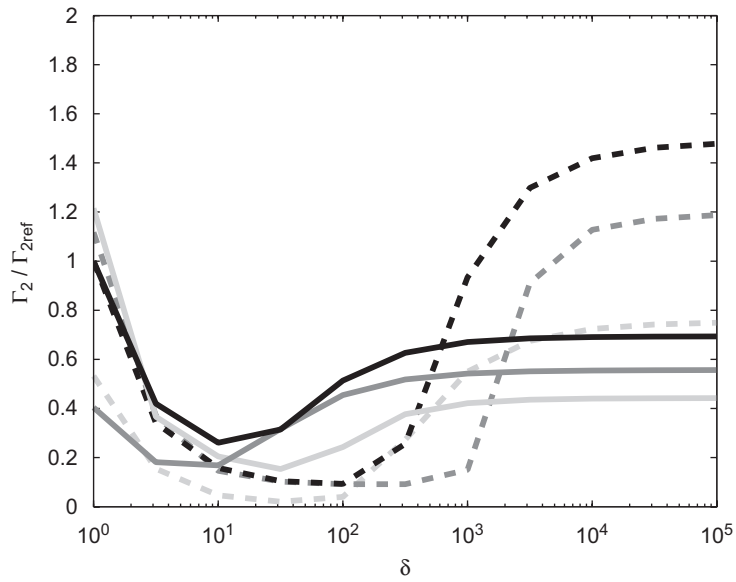


Fig. 6. Evolution of the second nonlinear coefficient Γ_{2222} with respect to the flexural rigidity ratio between outer and inner structures δ for different values of density ratio σ . Black lines represent the case where $\sigma = 0.1$, dark gray lines for when $\sigma = 1$ and light gray lines for when $\sigma = 10$. The results are normalized by the value Γ_{2ref} obtained in the limiting case where $\delta = \sigma = 1$. The dashed curves (— —) stand for the case $s = 0.9$ and the solid curves for the case $s = 0.7$. A minimum is reached when $10 < \delta < 100$ depending on the geometrical ratio s .

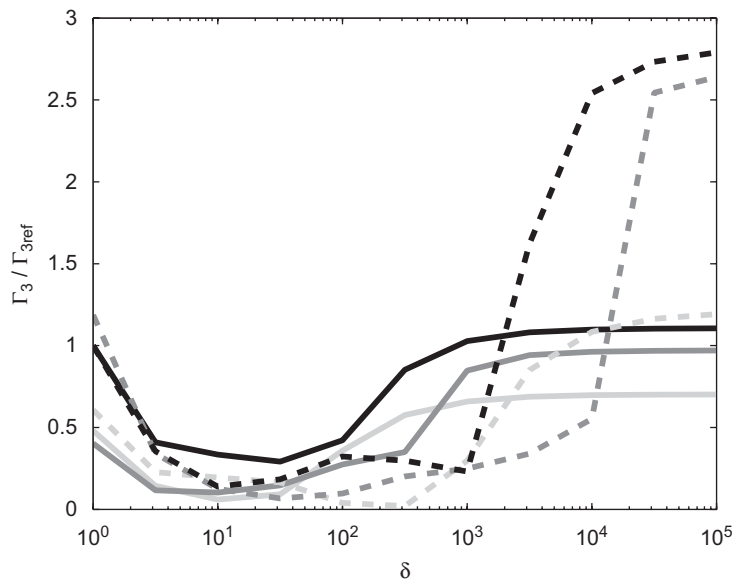


Fig. 7. Evolution of the third nonlinear coefficient Γ_{3333} with respect to the flexural rigidity ratio between outer and inner structures δ for different values of density ratio σ . Black lines represent the case where $\sigma = 0.1$, dark gray lines for when $\sigma = 1$ and light gray lines for when $\sigma = 10$. The results are normalized by the value Γ_{3ref} obtained in the limiting case where $\delta = \sigma = 1$. The dashed curves (— —) stand for the case $s = 0.9$ and the solid curves for the case $s = 0.7$. A minimum is reached when $10 < \delta < 100$ depending on the geometrical ratio s .

between oscillators a , p , q and r . It is therefore reasonable to study the coefficient Γ_{aaaa} only, since it is the only factor that contains the most pronounced nonlinear effect.

Figs. 5–7 represent the evolution of Γ_{aaaa} for the three first modes for different values of parameters δ and σ . All results are normalized by the value of Γ obtained when $\delta = \sigma = 1$.

As in the previous discussions on the eigenfrequencies, the first mode of vibration must be treated separately from the others, because δ only influences Γ_{1111} . On Fig. 5, it appears that the minimum for this nonlinear coefficient is reached when $\delta \simeq 30$, which corresponds to nearly a quarter of the value obtained in the “piston” case ($\delta \gg 1$). For the other modes of vibration, two regimes can be defined and are valid for all modes:

- For $\delta < 100$ the nonlinear coefficients depend only on δ and the minimum for Γ is reached for $\delta \simeq 30$.
- For $\delta > 100$ (piston approximation) the nonlinear coefficients are quite independent of δ and only the density ratio σ and the geometrical ratio s have an influence on the considered coefficients.

In the context of loudspeaker design, Figs. 5–7 show domains depending on δ and σ where the geometrical nonlinearities are reduced, thus allowing a better reproduction of sound for large amplitudes of the diaphragm. The condition where $\sigma = 10$ and $\delta = 30$ is an example of a good candidate.

5.5. Influence of the geometrical parameter s

Finally, we investigate the influence of the geometrical parameter s . The material properties are selected so that nonlinearities are as small as possible: in practice a value of $\delta = 30$ should be selected.

The influence of the geometrical parameter s on the two lowest eigenfrequencies ω_1 and ω_2 , and on the nonlinear parameters Γ are presented in Figs. 8 and 9 for 3 different values of σ .

These simulations show that the geometrical parameter s has a large influence on both the linear and nonlinear regime of vibrations, since it affects together the eigenfrequencies and the nonlinear coefficients. Fig. 10 shows the dependency of Γ_{1111} with s , and it can be seen that the nonlinear coefficient is reduced by a factor 100 between $s = 0.1$ and 0.9. This means that in the configuration when $s = 0.9$, the system is

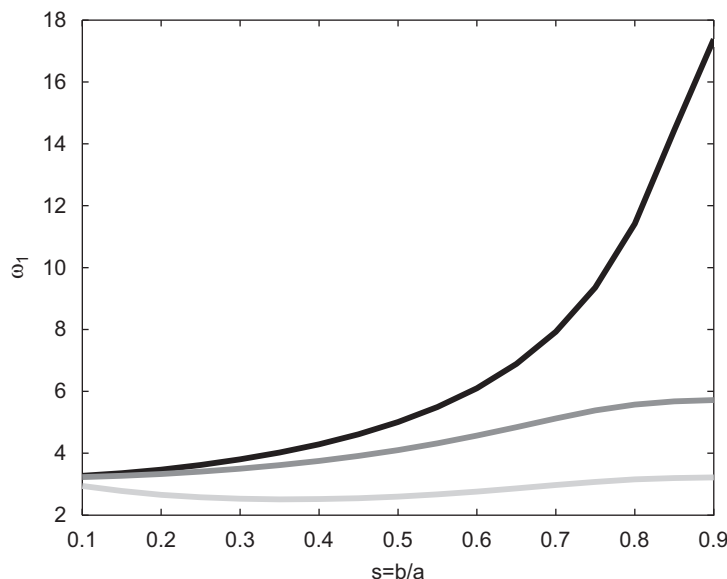


Fig. 8. Variations of the first angular frequency ω_1 of the structure versus the geometrical parameter s in the case where $\delta = 30$ for different values of density ratios σ . The black line represents the case where $\sigma = 10^{-1}$, the dark gray for when $\sigma = 1$ and the light gray when $\sigma = 10$. Except for low values of σ , s has little influence on the first eigenfrequencies.

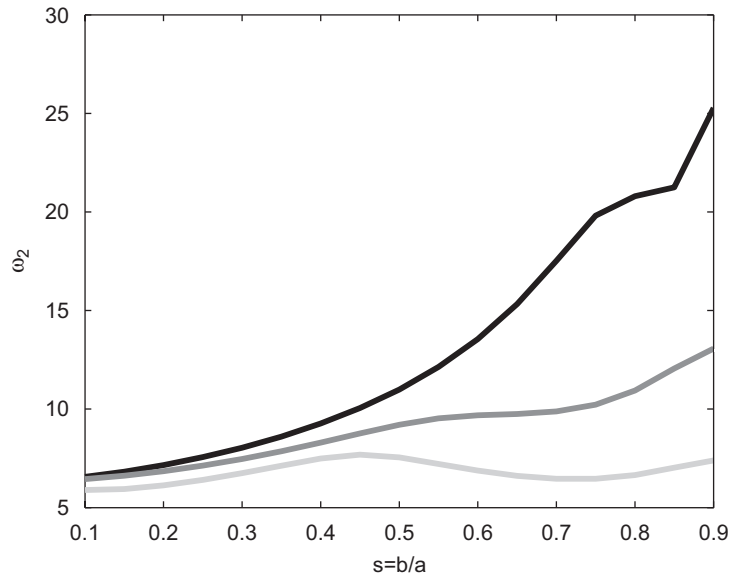


Fig. 9. Variations of the second angular frequency ω_2 of the structure versus the geometrical parameter s in the case where $\delta = 30$ for different values of density ratios σ . The black line represents the case where $\sigma = 10^{-1}$, the dark gray for when $\sigma = 1$ and the light gray when $\sigma = 10$. Except for low values of σ , s has little influence on the first eigenfrequencies.

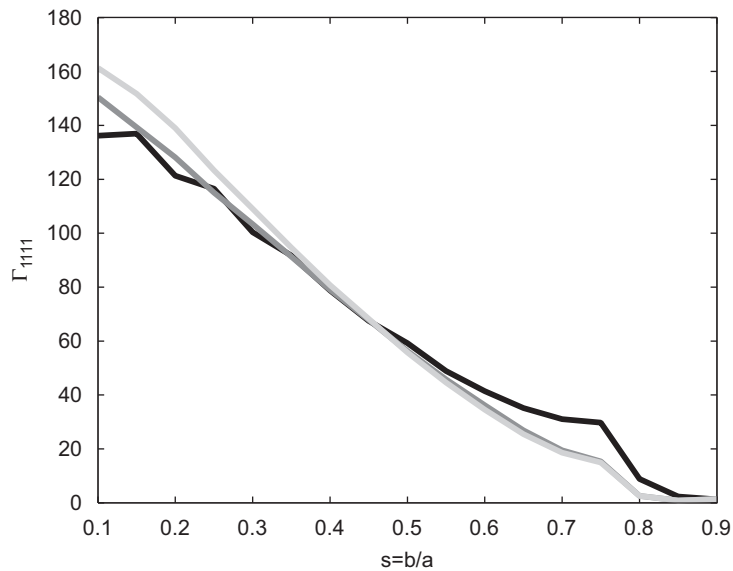


Fig. 10. Variations of the nonlinear coefficient Γ_{1111} for the first mode versus s for different values of σ in the case where $\delta = 30$. The black line represents the case where $\sigma = 10^{-1}$, the dark gray for when $\sigma = 1$ and the light gray when $\sigma = 10$. Independently of σ , the nonlinear coefficient of the first mode decreases with s . In order to reduce nonlinearities, the ratio of inner and outer diameters s must be chosen to be as low as possible.

almost linear and that high levels of vibration can be reached without distortion. The same tendency is observed numerically for higher modes of vibration: a minimum for Γ_{aaaa} is obtained when $s = 0.9$. Such considerations should be of help in the context of loudspeaker design (Fig. 11).

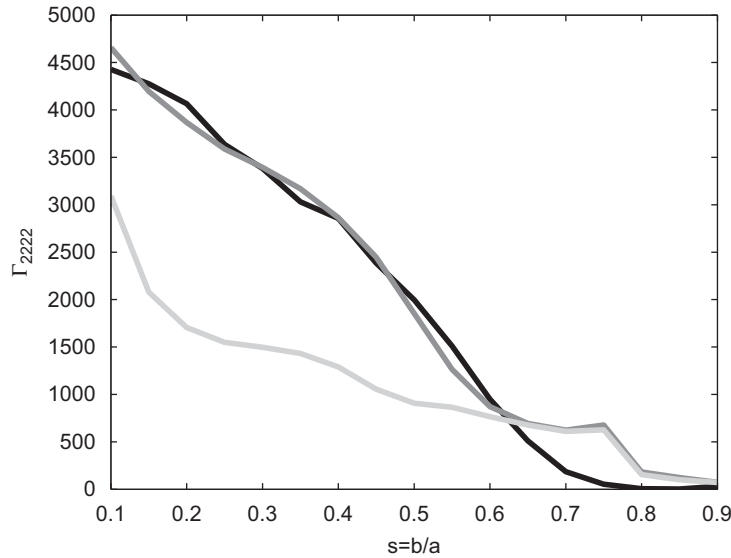


Fig. 11. Variations of the nonlinear coefficient Γ_{2222} for the second mode versus s for different values of σ in the case where $\delta = 30$. The black line represents the case where $\sigma = 10^{-1}$, the dark gray for when $\sigma = 1$ and the light gray when $\sigma = 10$. Independently of σ , the nonlinear coefficient of the first mode decreases with s . In order to reduce nonlinearities, the ratio of inner and outer diameters s must be chosen to be as low as possible.

6. Conclusions

Nonlinear vibrations of an idealized loudspeaker (viewed here as the combination of an annular suspension with a circular plate) were presented in this paper. The aim of this study was to investigate the role of geometrical and material parameters (density, flexural rigidity, thickness) in the vibrations of such structures. The leading idea behind this work was to determine whether appropriate selection of geometry and material could lead to significant reduction of commonly observed distortion in the reproduction of sound by electrodynamic loudspeakers.

It has been shown that the general formulation of the nonlinear problem is identical in form to the one of a plate (including cubic nonlinearities), provided that appropriate dimensionless parameters are introduced which represent the relative magnitudes of geometrical and material properties of both components of the structure. In the linear range, it has been shown that only the density and flexural rigidities ratios have an influence on the modal shapes and associated eigenfrequencies. It is also shown that nonlinearities are mostly related to the longitudinal and flexural rigidities ratio γ and δ . The application of our general method to the case of loudspeakers shows the existence of preferential geometrical and material configurations for the compound structure that reduce nonlinear effects commonly observed in real loudspeakers configurations.

Future developments of the model will include the effects of small curvatures on the central surface, responsible for an elevation of stiffness constants and for generation of quadratic nonlinearities observed in our experimental observations of loudspeaker subjected to large amplitude motions.

Appendix A. Modal shapes Φ_p and frequencies ω_p for the linear problem

A.1. Modal shapes

In this section, the nonlinear terms are neglected in Eq. (12). The force function is set to zero and no loading is present. The general equations for the compound structure ($A + B$) reduce to for $0 < r < s$:

$$\frac{\delta}{\sigma} \sum_{p=0}^{\infty} (\Delta \Delta \Phi_p(r)) q_p(t) + \sum_{p=0}^{\infty} \Phi_p(r) \ddot{q}_p(t) = \frac{\varepsilon}{\sigma} \left(-2\sigma\mu_B \sum_{p=0}^{\infty} \dot{q}_p(t) \Phi_p(r) \right) \quad (34)$$

for $s < r < 1$:

$$\sum_{p=0}^{\infty} (\Delta\Delta\Phi_p(r))q_p(t) + \sum_{p=0}^{\infty} \Phi_p(r)\ddot{q}_p(t) = \varepsilon \left(-2\mu_A \sum_{p=0}^{\infty} \dot{q}_p(t)\Phi_p(r) \right). \tag{35}$$

Considering a harmonic solution such as $q_p(t) \propto \cos(\Omega t)$, after projecting onto the p th mode, one obtains for $s < r < 1$:

$$\Delta\Delta\Phi_p(r) + \Omega^2\Phi_p(r) = -\varepsilon(2\mu_A j\Omega\Phi_p(r)) \tag{36}$$

for $0 < r < s$:

$$\frac{\delta}{\sigma}\Delta\Delta\Phi_p(r) + \Omega^2\Phi_p(r) = -\varepsilon(2\mu_B j\Omega\Phi_p(r)). \tag{37}$$

These equations can be solved with an expansion on the Bessel functions of the first and second kind for $0 < r < s$:

$$\Phi_p(r) = P_{1p}J_0(\zeta r) + P_{2p}Y_0(\zeta r) + P_{3p}I_0(\zeta r) + P_{4p}K_0(\zeta r) \tag{38}$$

for $0 < r < s$, the solution needs to be defined for $r = 0$:

$$\Phi_p(r) = P_{5p}J_0(\zeta \mathcal{L}r) + P_{6p}I_0(\zeta \mathcal{L}r) \tag{39}$$

with $\zeta^2 = \Omega$ and

$$\mathcal{L} = \left(\frac{\sigma}{\delta} \right)^{1/4}. \tag{40}$$

The modal shapes are then normalized using the following condition:

$$\iint_S \Phi_p^2 dS = 1.$$

A.2. Eigenfrequencies

Using the boundary conditions of our linearized problem, one can reformulate the problem in matricial form. We introduce

$$\mathbf{P}_p = (P_{1p} \ P_{2p} \ P_{3p} \ P_{4p} \ P_{5p} \ P_{6p}),$$

$$\mathbf{C}_p = \begin{pmatrix} J_0(\zeta) & Y_0(\zeta) & I_0(\zeta) & K_0(\zeta) & 0 & 0 \\ J_1(\zeta) & Y_1(\zeta) & -I_1(\zeta) & K_1(\zeta) & 0 & 0 \\ J_0(\zeta s) & Y_0(\zeta s) & I_0(\zeta s) & K_0(\zeta s) & -J_0(\zeta Ls) & -I_0(\zeta Ls) \\ J_1(\zeta s) & Y_1(\zeta s) & -I_1(\zeta s) & K_1(\zeta s) & -J_1(\zeta Ls) & I_1(\zeta Ls) \\ F_1(\zeta s) & F_2(\zeta s) & -F_3(\zeta s) & F_4(\zeta s) & -\delta LF_5(\zeta Ls) & \delta LF_6(\zeta Ls) \\ J_1(\zeta s) & Y_1(\zeta s) & I_1(\zeta s) & -K_1(\zeta s) & -\delta L^3 J_1(\zeta Ls) & -\delta L^3 I_1(\zeta Ls) \end{pmatrix},$$

where

$$\begin{pmatrix} F_1 \\ F_2 \\ F_3 \\ F_4 \\ F_5 \\ F_6 \end{pmatrix} = \begin{pmatrix} \zeta s J_0 - (1 - v_A^2) J_1 \\ \zeta s Y_0 - (1 - v_A^2) Y_1 \\ \zeta s I_0 - (1 - v_A^2) I_1 \\ \zeta s K_0 - (1 - v_A^2) K_1 \\ \zeta L s J_0 - (1 - v_B^2) J_1 \\ \zeta L s I_0 - (1 - v_B^2) I_1 \end{pmatrix}.$$

The boundary conditions can be rewritten in matrix form as

$$\mathbf{C}_p \cdot \mathbf{P}_p = 0. \quad (41)$$

This problem has no vanishing solutions under the condition:

$$\det(\mathbf{C}_p) = 0.$$

This equation has an infinite number of solutions $\zeta_p = \Omega_p^4$ and the eigenfrequencies are:

$$f_p = \frac{\Omega_p^2}{2\pi a^2} \sqrt{\frac{D_A}{\rho_A h_A}}. \quad (42)$$

The modal shapes are then solutions for Eqs. (38) and (39) for $\zeta = \zeta_p$.

References

- [1] W. Klippel, Diagnosis and remedy of nonlinearities in electrodynamic transducers, *109th AES Convention Los Angeles*, Preprint 5161, September 2000.
- [2] W. Klippel, Nonlinear large signal behavior of electrodynamic loudspeakers at low frequencies, *Journal of the Audio Engineering Society* 40 (1992) 483–496.
- [3] Z.L. Zhang, Q.T. Tao, Experimental study of nonlinear vibrations in a loudspeaker cone, *Journal of Sound and Vibration* 248 (2001) 1–80.
- [4] N.W. McLachlan, On symmetrical modes of vibration of truncated conical shells with application to loudspeaker diaphragms, *Proceedings of the Physical Society* 44 (1932) 408–425.
- [5] E.B. Skrodzka, A.P. Sek, Comparison of modal parameters of loudspeakers in different working conditions, *Applied Acoustics* 60 (2000) 267–277.
- [6] D.J. Murphy, Axisymmetric model of a moving-coil loudspeaker, *Journal of the Audio Engineering Society* 41 (1993) 679–690.
- [7] M. Petyt, P.N. G elat, Vibration of loudspeaker cones using the dynamic stiffness method, *Applied Acoustics* 53 (1998) 313–332.
- [8] O. Von Estorff, *Boundary Elements in Acoustics*, WIT Press, 2000.
- [9] A. Leissa, *Vibration of Plates*, Acoustical Society of America, 1993.
- [10] P.N. Raju, Vibrations of annular plates, *Journal of Aeronautical Society of India* 14 (1962) 37–52.
- [11] S. Azimi, Free vibration of circular plates with elastic edge supports using the receptance method, *Journal of Sound and Vibration* 120 (1988) 19–35.
- [12] P.A.A. Laura, G. Diez, V.H. Cortinez, A note on vibrating circular plates carrying concentrated masses, *Mechanics Research Communications* 11 (1984) 397–400.
- [13] S.A. Vera, M.D. Sanchez, P.A.A. Laura, D.A. Vega, Transverse vibrations of circular, annular plates with several combinations of boundary conditions, *Journal of Sound and Vibration* 213 (1998) 757–762.
- [14] C. Touz e, O. Thomas, A. Chaigne, Asymmetric nonlinear forced vibrations of free-edge circular plates, part 1: theory, *Journal of Sound and Vibration* 258 (2002) 649–676.
- [15] O. Thomas, *Analyse et Mod elisation de Vibrations Non-lin aires de Milieux Minces  Elastiques*, PhD Thesis, Universit e Pierre et Marie Curie, Paris VI, 2001.
- [16] S. Sridhar, D.T. Mook, A.H. Nayfeh, Nonlinear resonances in the forced responses of plates, part I: symmetric responses of circular plates, *Journal of Sound and Vibration* 41 (1975) 359–373.
- [17] J. Hadian, A.H. Nayfeh, Modal interaction in circular plates, *Journal of Sound and Vibration* 142 (1990) 279–292.
- [18] A.H. Nayfeh, D.T. Mook, *Nonlinear Oscillations*, Wiley, New York, 1979.
- [19] G. Handelman, H. Cohen, On the effects of the addition of mass to vibrating systems, *Proceedings of the Ninth International Congress Applied Mechanics*, Vol. 7, 1957, pp. 509–518.
- [20] S. Huang, Nonlinear vibration of a hinged orthotropic circular plate with a concentric rigid mass, *Journal of Sound and Vibration* 214 (1998) 873–883.
- [21] V. Ranjan, M.K. Ghosh, Transverse vibration of thin solid and annular circular plates with attached discrete masses, *Journal of Sound and Vibration* 292 (2006) 999–1003.
- [22] S.R. Li, Y.H. Zhou, X. Song, Nonlinear vibration and thermal buckling of an orthotropic annular plate with a centric rigid mass, *Journal of Sound and Vibration* 251 (2002) 141–152.
- [23] P.C. Dumir, C.R. Kumar, M.L. Gandhi, Nonlinear axisymmetric vibration of orthotropic thin annular plates with a rigid central mass, *Journal of the Acoustical Society of America* 77 (1985) 2184–2187.
- [24] A. Arpaci, Annular plate dampers attached to continuous systems, *Journal of Sound and Vibration* 191 (1996) 781–793.
- [25] M.F. Ashby, *Materials Selection in Mechanical Design*, Butterworth and Heinemann, Stoneham, MA, 2005.
- [26] O. Thomas, C. Touz e, A. Chaigne, Asymmetric nonlinear forced vibrations of free-edge circular plates, part 2: experiments, *Journal of Sound and Vibration* 265 (2003) 1075–1101.